RESEARCH INTO INDUCED BELT STRESS, LOCAL TO THE IDLER JUNCTION, DUE TO THE EFFECT OF IDLER SUPPORT CONFIGURATION

C. van der Linde[1], T. Frangakis[2]

[1] Flexco (Pty) Ltd
[2] School of Mechanical, Aeronautical and Industrial Engineering
University of the Witwatersrand

ABSTRACT

This paper presents preliminary data gathered from a purpose built test rig used in the research of conveyor belt idler junction failure. The results are the foundation for the broader aspects of this research in identifying the induced stress in the conveyor belt, local to the idler junction area. The research presented in this paper involved measuring the loads on the centre and wing idlers adjacent to the idler junction for a belt configured in a convex curve, in a static load case of tension only, and a pseudo-dynamic case of the tensioned belt being pulled over the idler sets at 60 mm/s. A single belt type (solid woven belt of class 1000) was tested using three idler configurations of varying offset (0, 150 and 240 mm) in conjunction with four troughing angles (0°, 15°, 25° and 35°). The preliminary results for the static case indicate that as the troughing angle is increased, the idler force increases (for both centre and wing rolls) while for particular troughing angles the centre and wing idler loads reduce as the offset distance is increased. The pseudo-dynamic case follows similar trends but has higher loads on the centre roll for the offset idler cases and for higher troughing angles, due to tension in the outer edges of the belt and distortion of the belt as it moves over the offset idlers.

INTRODUCTION

1.1. PURPOSE

The broad aims of this research project are to use a purpose built test rig (De Andrade, 2017) to investigate conveyor belt stress local to the idler junction, as a function of different idler configurations, belt type, trough angle and belt loading, all of which contribute to belt failures in this area. In addition, the test rig is configured as a convex curve which increases the belt stress in the junction.

1.2. MOTIVATION

It is widely known that conveyor belting is the most expensive component of conveyor systems (Zhang, 2015). To this extent, any form of failure including that attributed to the components in direct contact with the belt are of serious concern. Many forms of failure can occur and may be associated with the top or bottom cover, carcass and, in some cases, may be a propagating factor to each other.

In 2015, the Impumelelo conveyor in Secunda became the longest Overland Conveyor (OLC). Designed in partnership between ELB and an American based company, Conveyor Dynamics Inc. (CDI), the conveyor was seen as a major leap for conveying in the country, and in particular, the coal industry, which is heavily reliant on truck transport. The conveyor is just under 27 km in length, has varying horizontal curves and many elevation changes, and, in turn, vertical curves. During the design phase, a concern was raised with reference to damage of the conveyor belt in the idler junction area. The concern centred on the large spacing/pitch between idler sets which were designed to be on average 4.5 m. With this pitch being three times larger than the conveyor standard, an increase in belt sag was expected, as well as increased belt stress local to the junction area. In order to quantify the effects of the idler spacing, the Idler Junction Pressure Index (IJPI) was investigated by CDI. This idler junction pressure index is used to compare belt wear of a proposed design to known belt wear patterns at the idler junction, based on conveyor parameters such as belt speed, thickness, idler spacing, roll diameter etc. The magnitude of this parameter is used to give an indication of potential belt failure including degradation, spalling or worse, belt splitting (Thompson & Jennings, 2016). Based on the research, it was shown that the IJPI increased when the tonnage throughput, trough angle and idler pitch increased. The use of the IJP index value is applied by CDI and conveyor designers for both inline and offset idler configurations, and is a general value used in the conveyor design process.

2. LITERATURE REVIEW

Conveyor systems have been around since the late 18th century, where the first type of conveyor was used by farmers to move goods onto ships at port. It consisted of a simple leather belt running on a wooden base. Since this first mention of conveyors and belting, the system has gone through many evolutions and, in particular, the industrial revolution where Henry Ford made the conveying system famous in the production of the Ford Model T cars in 1913 (Concepts, 2014).

In the 100 plus years since then, there have been many advancements in conveyor technology particularly in the conveyor belt. During the early times of conveyor belts, the carcass was constructed of cotton duck and could require up to eight layers to get a tensile strength of 600 kN/m (Davies, 1981). The conveyor belting has improved to the thinner variants of today that can transport larger quantities of material over longer distances. These larger load quantities lead to localised stresses near the idler junction. The improvements in the carcass construction, in terms of materials and techniques, have resulted in far superior belts in both tensile strength and flexibility, as time moved on.

In the following sections, factors affecting belt stress in general as well as those highlighted to be a more direct aspect to idler junction stresses, will be explored. The custom design Idler Junction Failure (IJF) test rig will also be reviewed before the experimentation and preliminary results are presented.

2.1. STRESSES IN CONVEYOR BELTING

In general, there are many factors that contribute to stress within the conveyor belt. Most of these occur due to the dynamics of the belt cycling throughout the loop continuously. Stress may be induced in the belt due to factors such as:

- **Transition distance.** This is the distance between the head or tail pulley and the first set of idlers of full trough angle on the carry side. A short transition distance will cause the belt to fold quickly and lead to higher stresses at the idler junction. It will also lead to excessive stress in the belt edge due to the longer travel distance of the edge compared with the centre of the belt (Fenner-Dunlop, 2009).
- **Material load (active and passive stress states).** The material load in the trough causes the belt to open between idlers (active material stress state) and

close (passive material stress state) when in contact with the idler sets (Ilic, et al., 2017). The force required to displace the material between these two states adds loading to the idler and the belt.

- **Starting and stopping conditions.** A spike in tension during start-up induces substantially more internal stresses, while stopping may cause a rapid belt relaxation. Doing either of these too regularly (usually they accompany each other), stretches the belt and approaches the elastic limit at a faster rate. This is pronounced if there is no gradual start up sequence or lagging on the drive pulley.
- **Idler spacing**. This is the longitudinal spacing between idler sets and is directly related to the belt sag variable. A desired value of less than 2% belt sag is recommended, and can be accounted for with increased belt tensions (Fenner-Dunlop, 2009). Larger idler spacing also results in higher loads on both the idler and the belt in contact with the idler. This results in larger stresses and is particularly relevant to stresses in the idler junction area.
- **Minimum pulley diameter**. The smallest pulley diameter the belt will encounter is important to selecting the correct belt. Additional tension is imparted into the carcass and the plies as the belt bends around the circumference of the pulley. Essentially the top cover and carcass stretch further while the bottom cover is compressed (Figure 1). A smaller pulley diameter implies more bending and stretch in the carcass which may push the belt closer to the shear stress limit of the ply bonding. If not designed correctly, failure from this includes premature splice failure and ply separation. Separation of plies significantly weakens the strength of the belt and may aid in junction failures (Dunlop Belting, n.d.).

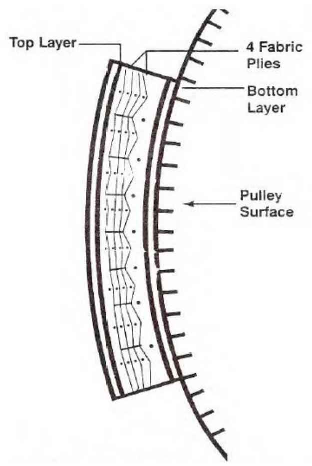

Figure 1: Ply Separation Failure due to Increased Stress around the Pulley (Dunlop Belting, n.d.)

2.2. IDLER JUNCTION FAILURE (IJF)

In the past, when conveyor belting was designed for increased strength, the tendency was to reduce the belt thickness. With increased strength and a demand for higher conveyor throughput, their loading capacities also increased. This played a role in squeezing the belt into the gap between inline idlers (Figure 2), which resulted in the belt being pinched at the junction. This pinching action occurs in the gap between the centre and wing rolls. The idler spacing at this location therefore may also have an effect on the failure occurrence at the junction. The alternate offset idler configuration (such as the SANS 1313 configuration with a 150 mm offset) was developed in order to mitigate this pinching behaviour.

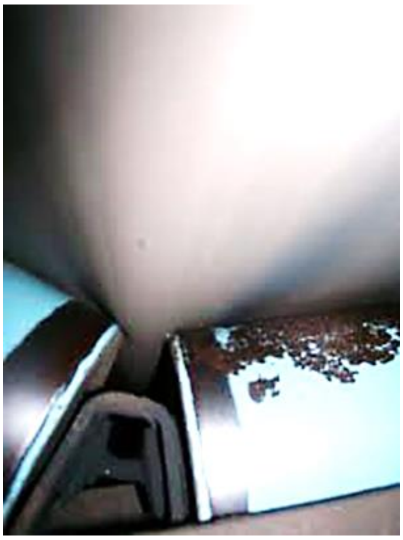

Figure 2: Pinching of the belt in the idler junction - inline configuration (Zhang, 2015)

The dynamic effects of the conveyor system, however, have a drawback associated with the offset configuration. Due to the centre idler being located upstream of the wing rolls, the belt is essentially lifted by the centre roll first (while still open at the edges in the active material stress condition, Ilic et al., 2017) and then supported by the wing rolls thereafter. Essentially, the offset configuration does not support the belt across the complete width of the belt at a particular transverse cross-section and, when loaded, the belt distorts (or “creases”) between the idlers (Figure 3), which may contribute to junction failure.

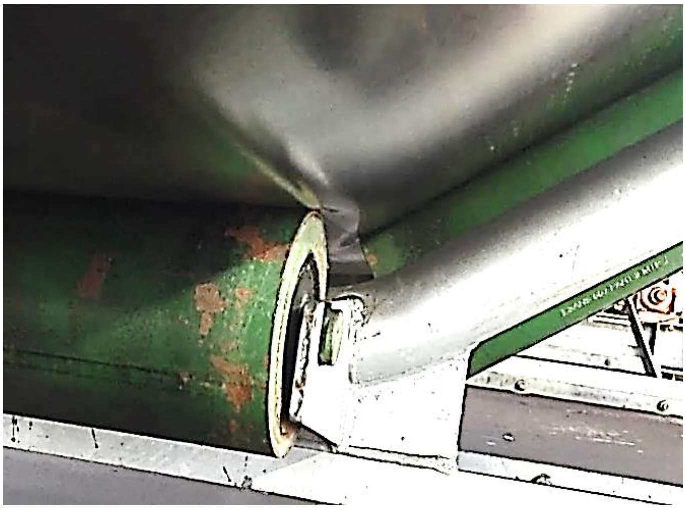

Figure 3: Belt friendly idler frame - creasing of the belt between the idlers (Kruse, 2019)

The development of the “belt friendly” idler configuration (with an increased offset between centre and wing rolls of 240 mm) has seen a heavy utilisation in industry with low levels of research to support its perceived benefits. The increased offset results in a change in the material surface profile as it passes through the idler junction (Figure 4), which is indicative of internal material shear that would impart contact stress to the belt. Additionally, this material shifting results in the belt undergoing rapid directional changes through the junction area.

Given the repetitive load shifting and directional belt changes throughout the conveyor cycle, large internal bending and shear stresses may form in the conveyor belt at this point.

Figure 4: Material shifting as it moves over the offset idlers (Frittella, 2018)

There are several aspects to consider when researching belt failure around the idler junction. Some of these are the main focus of this study and include:

- **Idler configuration**. An offset configuration is seen to reduce the bending stress in the belt and pinching potential, however, dynamically is seen to induce material shifting and creasing in the belt, with associated belt stress. The 3-roll troughing variations of inline and offset idlers lead to stress concentration points local to the idler junction. A 3-roll trough has three surfaces of belt support with localised loads on these surfaces and has two points of angle change (with associated stress). Research has been carried out into a 5-roll troughed configuration which produces a cross-section more conforming to the natural flexure shape of the belt than a 3-roll configuration (Elliot, et al., 2015). However, this 5-roll configuration consists of multiple offset idlers which increases the number of junction and local directional changes in the belt.
- **Trough angle**. Lower trough angles would imply a lower belt capacity and thus reduced load that is supported by the idlers. Up to a certain point, an increasing trough angle increases the load carrying capacity (Human & Nel, 2011). A by-product however of an increased trough angle is the extra folding of the belt in the weft direction local to the idler junction. This increase in load carrying capacity also increases load central to these critical junction points and increases the potential of pinching the belt between idlers of the inline configuration. It also increases material mass that undergoes changes in profile in relation to the use of offset idlers, thereby increasing belt loads.
- **Conveyor shape.** This aspect refers to the convex curves that exist in many conveyor transitions from an incline to a level belt (Figure 5) as well as in mobile stacker-reclaimers. The convex curve increases the tension in the outer troughed sections of the belt and increases the likelihood of pinching or belt distortion in the junction area. The convex shape cannot be perfectly rounded and is instead a series of straight belt sections creating the convex shape.

Figure 5: Convex Shape and Indentation of belt over Idlers

- **Belt thickness**. A thicker belt carcass may have more transverse strength and rigidity to resist belt pinch between the inline rolls, however reduced bending capabilities in the weft direction to fill the trough shape. Thinner carcass belts may have less transverse weft strength and rigidity, thus making them more susceptible to ply delamination.
- **Belt characteristics**. Different belting types (solid woven and multi-ply) will have different strength characteristics. A belt with a lower transverse stiffness may not bridge the roll gap sufficiently (Figure 2) and be pressed into the gap between the idlers (leading to pinching).

Other factors may contribute to junction failure such as transition distances, loaded material characteristics and idler spacing. Although valid, these parameters are outside the scope of this preliminary research.

2.3. SCOPE AND OBJECTIVE

The preliminary research presented in this paper will focus on forces measured in idler sets arising from the following variables:

- Idler offset ranging from 0 mm to 240 mm;
- Idler trough angle from 0° to 35°;
- Solid woven belting of class 1000 rating.

The objectives of the present research are to:

- Measure the loading on the centre and wing idlers associated with inline and offset configurations, under static and pseudo-dynamic conditions.

3. IJF RIG

3.1. OVERVIEW

The purpose-built rig for this study was designed to replicate the extreme case of belt compression on the idlers in a convex curve (such as that shown in Figure 5). The rig is capable of using a maximum belt width of 1050 mm and idler face length of 390 mm. The convex curve radius is approximately 35 m with the idlers nominally spaced at 1.3 m intervals. Variables may include idler configuration (0, 150 and 240 mm offsets), trough angle (0°-90°), idler configuration spacing and idler dimension (127 and 152 mm diameters). The design is "quasi-static" in that the belt is fixed at its ends and only moved a fixed amount of 1.2 metres. It may be loaded with material to simulate a more real world application (De Andrade, 2017). Through a loaded belt condition, the prevalence of bottom cover belt deformation will increase.

A tensioning device consisting of a hydraulic power pack and two hydraulic cylinders in parallel provide the force required to tension the belt to a tension of approximately 18 - 19 tonnes. The tension is transmitted to the conveyor belt through steel wire rope cables running through a series of sheaves and connected to a bogie and belt clamp, which is fastened to the belt through mechanical fasteners. Post belt tensioning, a bi-directional winch moves the trolley along a set of rails in either direction (Figure 6), allowing the belt to traverse a distance of 1.2 m, at a rate of approximately 60 mm/s.

(a)

(b)

Figure 6: Hydraulic cylinders providing belt tension mounted to a trolley; (b) Winch system moving the trolley

A take-up and two turnbuckles are used in order to apply a pre-tension to the belt before the hydraulic cylinders tension the belt to its preset tension value
(
Figure 7).

Figure 7: Take-up and Turnbuckle used to Pre-Tension the Belt

Data collection is in the form of load cells placed under the idler rolls at three locations: the idler set at the apex of the convex curve, and the idler sets directly upstream and downstream thereof (Figure 8 and Figure 9). An additional load cell (20 tonne maximum) is used to measure the belt tension and is located on the rope connection to the bogie, on the one side. The loads determined at the idlers are also experienced in the belt at the interface of belt and idler, and will be used in further research in a Masters project to assess belt stress. All the load cell readings are captured through the data acquisition system and reported in units of kilogram force.

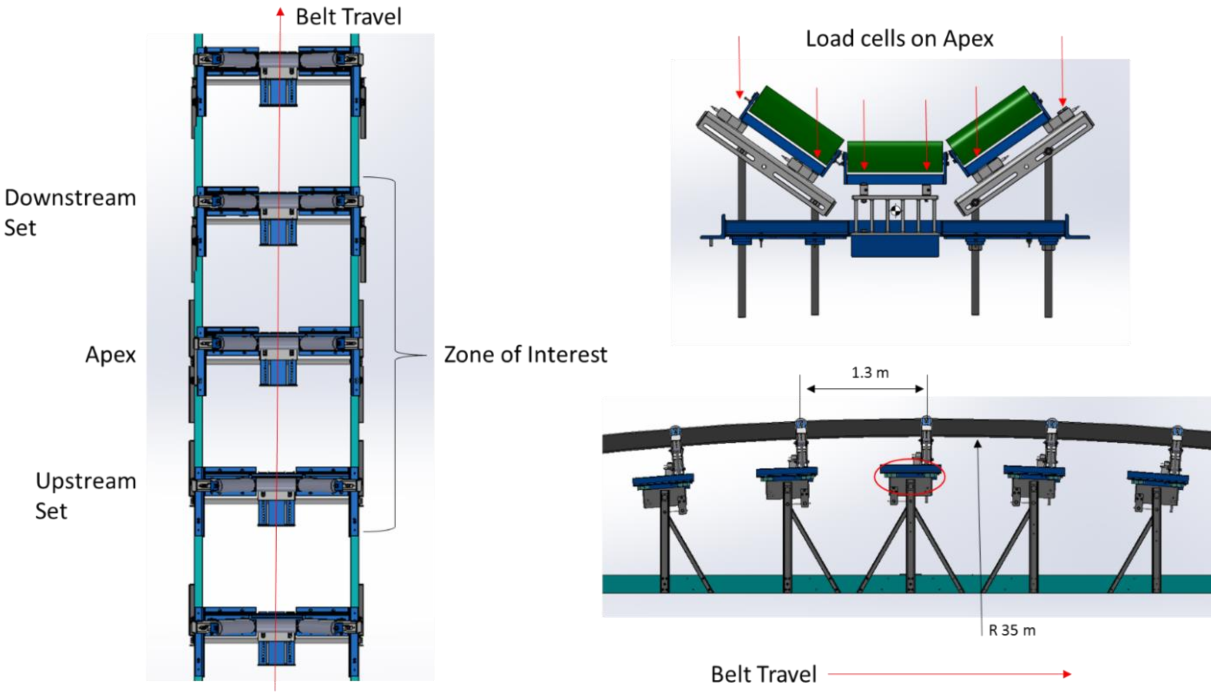

Figure 8: Load cells in the zone of Interest

(a) (b)

Figure 9: (a) Tension Load cell; (b) Idler Load Cell Placement.

3.2. TEST METHOD

For each configuration of test variables, a static and pseudo-dynamic test was performed on a solid woven belt of class 1000 rating. The static analysis included tensioning the belt to maximum of 18 - 19 tonnes while simultaneously recording the loads of all load cells. The tension was maintained for 30 s during which the loads were recorded as belt relaxation was expected to occur. The maximum loads experienced by the loadcells during this 30 s period were recorded. The tension was then released. In the pseudo-dynamic tests, the belt was tensioned as before, after which the belt was moved at 60 mm/s for approximately 20 s. The loads on the idlers was recorded for the 20 s duration and all of the data was then averaged.

Table 1 shows the test configurations where the trough angle and idler type (i.e. offset distance) were varied. While not practical, a zero wing roll angle was included in the test programme for comparison. Each configuration was tested three times as per the above procedure.

Table 1: Test programme

Test Number	Wing Roll Angle (°)	Offset Distance (mm)	Idler Gap / Overlap (mm)
1 (Baseline)	0	0	60
1 (Baseline)	0	150	10
1 (Baseline)	0	240	10
2	15	0	40
3	25	0	30
4	35	0	15
5	35	150	10
6	25	150	10
7	15	150	10
8	15	240	10
9	25	240	10
10	35	240	10

Since the idler loads in the centre and wing rolls adjacent to the junction area are indicative of the belt loads in that area, the processing of the loadcell data was as follows:

- For the **static case,** the maximum load recorded on each load cell was recorded for the centre and wing idlers. The maximum readings of the loadcells local to the junction area, both inboard (centre rolls) and outboard (wing rolls), were then averaged over the three idler sets. This is depicted schematically in Figure 10.
- For the **pseudo-dynamic case**, readings of all the centre and wing roll loadcells (which amounted to 20 s worth of data for each of the three tests per configuration), were averaged across the three idler set loadcells.

The rationale for averaging the readings is that the idler set geometries and longitudinal spacing thereof have minor variations, and there is also variation in the tension across the belt width due to differences in the belt clamp attachments and alignment. Since the belt tensions are also not constant throughout a test, and are not identical from test to test, the individual loadcell results are normalised against an average tension value.

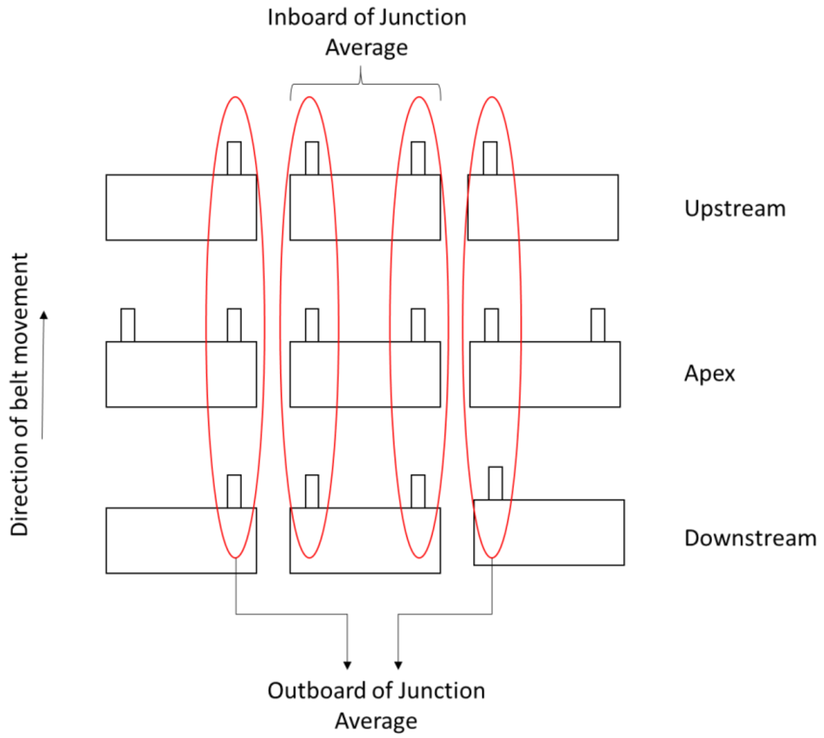

Figure 10: Post data processing diagram - inline depiction

4. RESULTS

The results of the **static loading case** are depicted in Figure 11 and Figure 12, for the centre and wing rolls respectively, as a function of offset distance and troughing angle. The inset numbers on each bar represents the average of the maximum loadcell readings in kilograms force while the error bars represent the maxima and minima of the averaged data for each of the 18 data sets per test configuration. The tabulated data is available in the Appendix.

The average load on the centre idler, inboard of the junction, shows a generally decreasing trend as the offset increases, for all troughing angles. A similar general trend is seen on the average loads on the wing idlers, outboard of the junction. With increasing offset, the centre idler supports a larger average load than the wing idler for all trough angles.

As the troughing angle increases, the average wing roll load increases for all offset configurations. A generally similar trend is seen in the centre roll loads but it is not as pronounced.

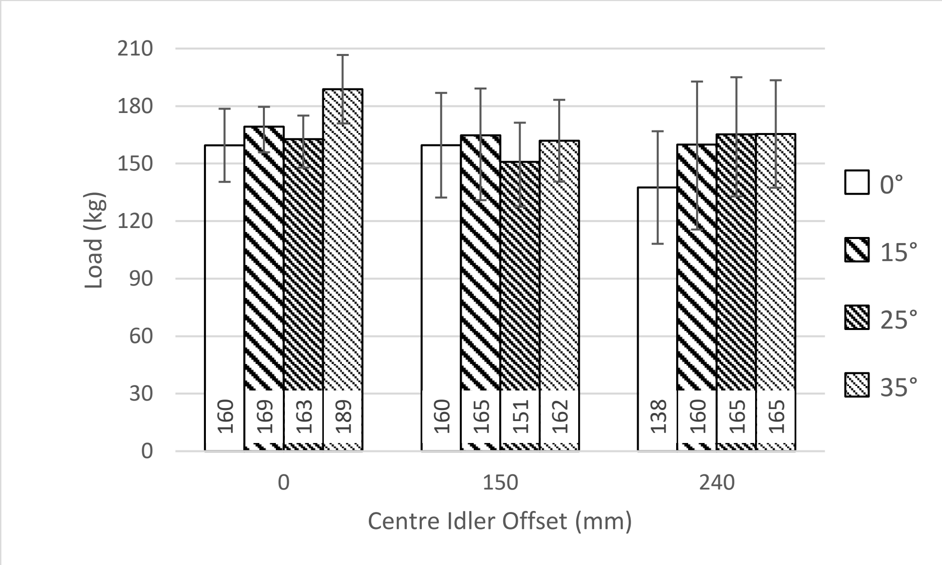

Figure 11: Average centre idler loads of all troughing angles and idler offset - static loading case

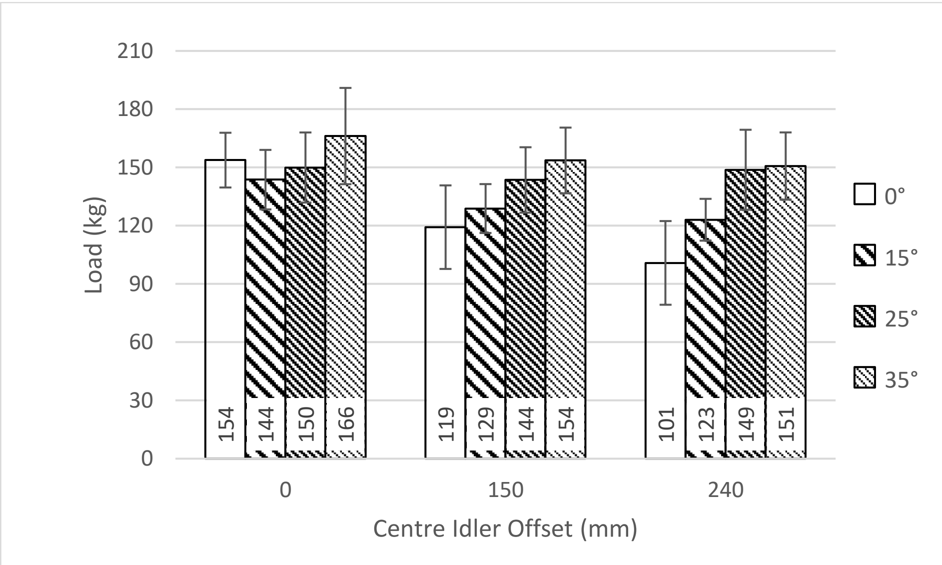

Figure 12: Average wing idler loads of all troughing angles and idler offsets - static loading Case

Figure 13 and Figure 14 show the results of the **pseudo-dynamic case** for the centre and wing idler rolls respectively. As with the static loading, the results show a similar trend for both the centre and wing idlers. The centre roll loads for a particular troughing angle tend to decrease with increasing offset (for the higher troughing angles), while loads for a particular offset increase as the troughing angle increases. The average values of the centre roll loadcell readings for the 25 and 35° troughing angles are typically of the order of 10% higher than those of the static case. However, the opposite effect is seen in the wing rolls for the 25 and 35° troughing angles, where the average loads reduce slightly.

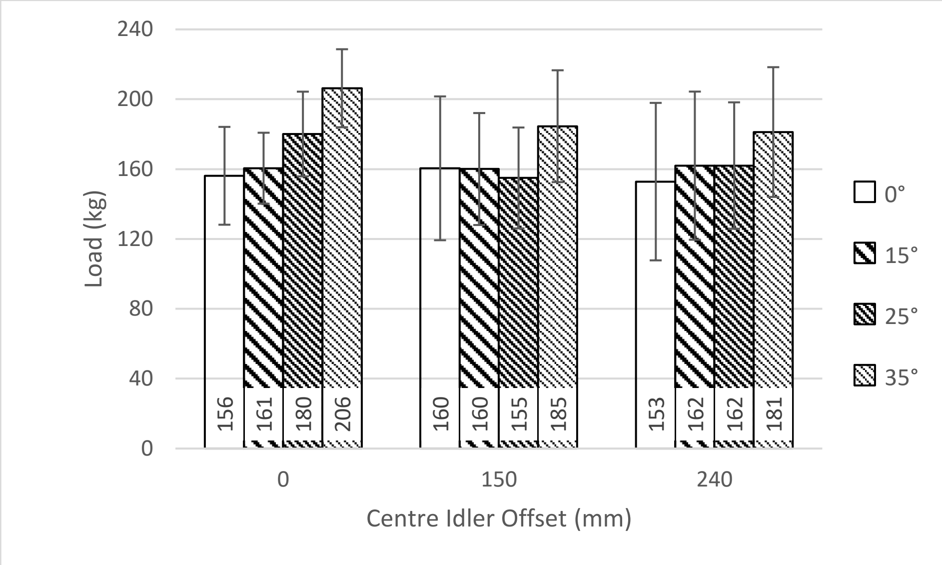

Figure 13: Average centre idler loads of all troughing angles and idler offset - pseudo-dynamic loading case

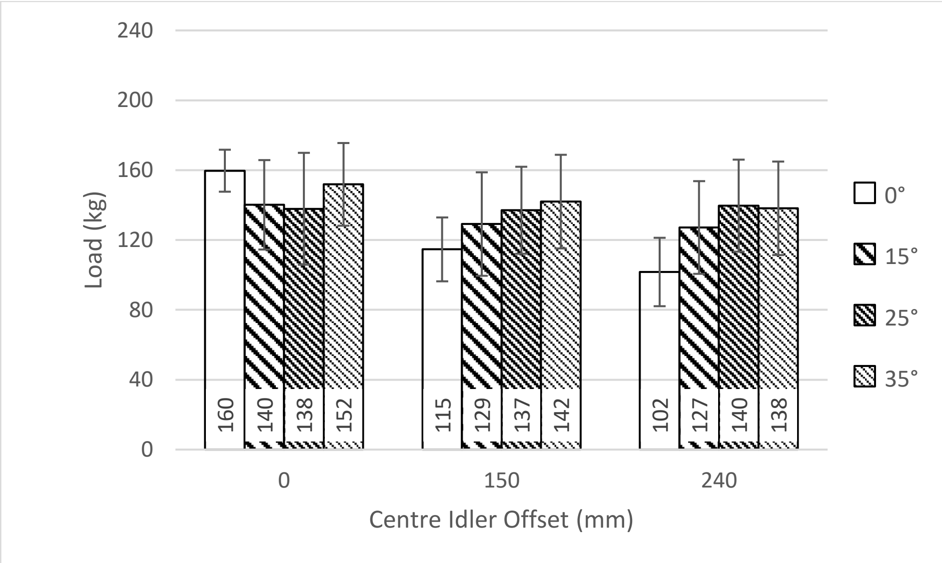

Figure 14: Average wing idler loads of all troughing angles and idler offset - pseudo-dynamic loading case

5. DISCUSSION

The objective of this testing was to obtain preliminary results of idler forces from the convex curve test rig. The scope of testing was limited to one type of belt construction (solid woven) with a width of 1050 mm and a belt tension of 18.5 tonnes. The parameters of the test covered three different offset configurations namely inline (0 mm offset), SANS 1313 industry standard (150 mm offset) and a commonly used "belt friendly" configuration (240 mm offset). All three configurations were subject to testing over four trough angles (0°, 15°, 25° and 35°).

Each of the test configurations was repeated three times, with data from six centre and six wing idlers being recorded per test. A static test was conducted where the belt was tensioned for a period of 30 seconds during which the maximum loadcell readings were recorded for each loadcell. The maxima of the six centre loadcells were averaged, as were the maxima of the six inner loadcells of the wing idlers. Pseudo-dynamic tests were also conducted where the belt was tensioned and then pulled over the idler sets at a speed of 60 mm/s, for a duration of 20 seconds. This data was also averaged to yield centre and wing roll loads adjacent to the idler junction. In addition, since the belt tensions could not be replicated identically from test to test, results of tests were normalised against average tension values.

For the **static** case, the average load on the centre idler showed an increasing trend as the troughing angle increased. This is possibly due to the higher tension towards the edges of the belt as the troughing angle is increased. The higher tension at the belt edges is due to the effect of the convex curve and the location of the edge relative to the curve. This would possibly result in compressive forces towards the centre section of the belt, which would be predominantly be reacted by the centre roll.

For a particular troughing angle there was also a general decrease in load on the centre roll as the offset increased. Considering an inline troughed idler case, the change in angle of the belt as it traverses the idler set results in high tension in the outer edges of the belt as the transition occurs over a short distance. As the offset is increased, the angle of the belt is changed over the offset distance and not at a single location, so it is reasonable to expect the effect of the tension in the outer portions of the belt is ameliorated to some extent, which could reduce the loads experienced by the centre roll.

Similar trends are seen in the wing rolls. The tension in the outer edges of the belt plays an increasing role as the troughing angle is increased. There is also more belt in contact with the wing rolls as the troughing angle is increased, which may also contribute slightly to the reduction in load on the centre roll. At present, data was not acquired to the same extent for the outer loadcells of the wing rolls (as only two loadcells were available for this purpose). It is proposed for future tests to account for the loads on all six outer loadcells as well to better understand the change in load as the offset and troughing angles are increased.

For the **pseudo-dynamic** case, similar general trends were observed for both the centre and wing rolls as with the static case. Increasing troughing angle increases the wing roll forces, while increasing the offset distance decreases the wing roll forces. However, when compared with the static case, the centre roll loads increased for the 25 and 35° troughing angles, while the wing rolls showed decreases for these troughing angles. Since the belt passes the centre roll before the wing rolls in the offset configurations, the distortion of the belt as it moves over the offset junction, in addition to the effects of tension in the outer portions of the belt (and the associated compressive forces towards the centre of the belt), result in increased resistance of the belt, and thus increased loads on the centre rolls.

The belt encounters the wing rolls after it has already encountered the centre roll when in motion. Since the centre roll experiences higher loads, it is reasonable that the wing rolls are partially unloaded and the load experienced is reduced slightly.

The traverse speed of the belt was limited by the winch speed to 60 mm/s. This is nowhere near the speeds encountered on practical conveyors, and the effect of belt inertia and material loading in the junction area, particularly when the belt distorts in relation to the use of an offset idler, is unknown. The current test rig is not able to conduct tests at higher loads, and an instrumented test of an operational conveyor would have to be undertaken to assess this effect.

The error bars shown in Figures 11 to 14 were specified on the basis of the range of values of the averages of each of the 18 data sets, rather than on the basis of standard deviations. This was done in order to show that there are significant differences in the test results from test to test. A standard deviation approach was not used due to the limited number of data points. The effect of belt stretch and subsequent loss of tension cannot be avoided during the 20 to 30 seconds of data acquisition, hence the use of average values of the loads and normalising of the data to an average tension value.

6. CONCLUSIONS AND RECOMMENDATIONS

A convex curve test rig sponsored by the CMA was commissioned. It was used to obtain preliminary forces on centre and wing rolls for a solid woven belt of class 1000, in a convex curve configuration of radius approximately 35 m. Three different idler configurations were tested including inline, SANS 1313 (150 mm offset) and “belt-friendly” (240 mm offset), each of which was tested with troughing angles including 0, 15, 25 and 35°.

Idler forces adjacent to the idler junction were measured and averaged for the centre roll and wing roll. Static tests were conducted at a nominal belt tension of 18.5 tonnes. A series of pseudo-dynamic tests were also conducted where the belt was tensioned and then pulled over the idler sets at a speed of 60 mm/s for a period of 20 s.

The results showed that increasing troughing angles result in generally increased centre and wing roll loads, and that increasing offsets results in generally decreasing static loads on the centre rolls, for particular troughing angles.

The pseudo-dynamic tests showed an increase in the loads on the centre roll for the higher troughing angles (25 and 35°), and a slight reduction in the loads on the wing rolls for the same troughing angles. There was also an increase in the centre roll loads as compared with the static case for the higher troughing angles.

Future work should include loadcells on the outer edges of all the wing roll sets, and could include a different belt construction, a loaded belt case, and possibly higher speeds for the pseudo-dynamic case.

It is also intended to measure the belt profile in the region of the idler set (for different offset configurations) to assess the effect of belt distortion and its potential contribution to belt stress.

7. ACKNOWLEDGEMENTS

I would like to extend my appreciation to Flexible Steel Lacing Company (Flexco RSA) in providing the means to undertake this project. Thanks also go to the contributing companies for rig development and supply of ancillary equipment, including Cowles Engineering, University of the Witwatersrand and Dymot. The Conveyor Manufacturers Association (CMA) is also thanked for their ongoing financial support of the project.

8. REFERENCES

1. Concepts, P. H., 2014. *The History of Conveyors,* s.l.: s.n.
2. Davies, G., 1981. Aspects of Conveyor Belting. *Beltcon*.
3. De Andrade, N., 2017. *Optimisation of the Offset Distance Between Idler Rolls to Minimise Stress Within COnveyor Belting,* JHB: s.n.
4. Dunlop Belting, n.d. *Conveyor Belt Design Manual,* s.l.: CKIT.
5. Elliot, M., James, G., McLennan, G. & Molden, P., 2015. *Conveyor Five (5) Roll Trough Idler Geometry Optimisation,* s.l.: Continental.
6. Fenner-Dunlop, 2009. *Conveyor Handbook.* s.l.:s.n.
7. Fenner-Dunlop, n.d. *Conveyor Belt Manual.* s.l.:s.n.
8. Frittella, A., 2018. *Material shifting and idler junction failure* [Interview] (02 August 2018).
9. Human, P. & Nel, P., 2011. *Conveyor Idler Troughing Profiles.* JHB, Conveyor Manufacturers Association.
10. Ilic, D., Wheeler, C. & Ausling, D., 2017. *Bulk Solids and Conveyor Belt Interactions During Transport.* s.l., IMHC.
11. Kruse, D., 2019. *Modelling in FEA* [Interview] (07 05 2019).
12. Thompson, M. & Jennings, A., 2016. Impumelelo Coal Mine. In: *Mining Engineering Magazine.* s.l.:s.n., pp. 14-35.
13. Wheeler, C., Roberts, A. & Jones, M., 2004. Calculating the Flexure Resistance of Bulk Solids Transported on Belt Conveyors. *Particle & Particle Systems Characterization,* 21(4).
14. Zhang, Y., 2015. *Conveyor Belt Bottom Cover Failure from Idlers and Pulleys.* s.l., International Materials Handling Conference (IMHC).

ABOUT THE AUTHORS

CARL VAN DER LINDE

BSc Mechanical Engineering (Honours), University of the Witwatersrand, 2015.

3 Years work experience with Flexco in the conveyor industry and working towards an MSc in mechanical engineering.

Carl van der Linde

Flexco PTY (LTD)

236 Albert Amon RD,

Meadowdale Ext 7,

Germiston 1614

South Africa

TEL: +27 011 608 4180

Email: cvanderlinde@flexco.com (Carl_VDL@hotmail.com)

TERRANCE FRANGAKIS

Terrance is a senior lecturer at the School of Mechanical, Industrial and Aeronautical Engineering at the University of the Witwatersrand, Johannesburg. He completed a Masters degree at Wits University, before working for six years as a project engineer in the mine mechanisation research area at the Mining Technology division of the CSIR. This was followed by six years as a project engineer at Novatek Drills, where he worked on the development of commercial pneumatic and hydraulic drilling equipment for the mining industry. He then joined the School of Mechanical, Industrial and Aeronautical Engineering in 2007 and has lectured courses in mechanical vibrations, mechanical engineering design and applied mechanics. For the last seven years, Terrance has been involved in research in bulk materials handling in association with the TUNRA Bulk Solids Africa laboratory at Wits University, which was established in collaboration with TUNRA Bulk Solids at the University of Newcastle, Australia. He is busy with a part time PhD in bulk materials handling.

Terrance Frangakis

Senior lecturer
School of Mechanical, Industrial and Aeronautical Engineering
University of the Witwatersrand
P/Bag X3, WITS, 2050, South Africa
Telephone: +27-11-717-7333
Email: Terrance.Frangakis@wits.ac.za

APPENDIX

Table 2: Average data readings for the Static inline configuration

Trough Angle	Wing Idler - Outbound of Junction			
	Average (kg)	Max (kg)	Min (kg)	Range (kg)
0°	153.766	171.468	136.050	35.419
15°	143.714	159.440	124.168	35.272
25°	149.955	172.374	126.796	45.578
35°	166.161	198.533	128.919	69.614
	Centre Idler - Inbound of Junction			
	Average (kg)	Max (kg)	Min (kg)	Range (kg)
0°	159.541	175.315	129.192	46.122
15°	169.272	180.151	155.908	24.243
25°	162.839	180.085	147.883	32.201
35°	188.802	209.257	168.810	40.448

Table 3: Average data readings for the static 150 mm offset configuration

Trough Angle	Wing Idler - Outbound of Junction			
	Average (kg)	Max (kg)	Min (kg)	Range (kg)
0°	119.238	151.251	99.407	51.844
15°	128.829	146.952	110.943	36.009
25°	143.543	175.957	127.731	48.226
35°	153.594	170.538	132.214	38.324
	Centre Idler - Inbound of Junction			
	Average (kg)	Max (kg)	Min (kg)	Range (kg)
0°	159.583	201.295	134.217	67.078
15°	164.752	189.029	130.935	58.094
25°	150.840	181.876	127.529	54.347
35°	161.901	185.993	134.800	51.193

Table 4: Average data readings for the static 240 mm offset configuration

Trough Angle	Wing Idler - Outbound of Junction			
	Average (kg)	Max (kg)	Min (kg)	Range (kg)
0°	100.826	132.088	78.191	53.898
15°	123.050	133.757	108.217	25.540
25°	148.786	188.603	131.992	56.611
35°	150.725	169.087	130.985	38.102
	Centre Idler - Inbound of Junction			
	Average (kg)	Max (kg)	Min (kg)	Range (kg)
0°	137.526	182.902	109.712	73.190
15°	159.978	206.019	115.622	90.398
25°	165.288	207.513	132.902	74.611
35°	165.438	203.574	133.938	69.636

Table 5: Average data readings for the pseudo-dynamic inline configuration

Trough Angle	**Wing Idler - Outbound of Junction**			
	Average (kg)	Max (kg)	Min (kg)	Range (kg)
0°	159.671	178.811	148.273	30.538
15°	140.147	166.355	106.720	59.635
25°	137.882	174.475	94.352	80.123
35°	151.858	177.574	111.944	65.630
	Centre Idler - Inbound of Junction			
	Average (kg)	Max (kg)	Min (kg)	Range (kg)
0°	156.157	185.324	113.096	72.228
15°	160.504	178.904	125.323	53.581
25°	180.090	205.827	143.355	62.471
35°	206.310	239.528	170.808	68.720

Table 6: Average data readings for the pseudo-dynamic 150 mm offset configuration

Trough Angle	**Wing Idler - Outbound of Junction**			
	Average (kg)	Max (kg)	Min (kg)	Range (kg)
0°	114.629	141.970	97.208	44.762
15°	129.135	168.942	96.100	72.842
25°	137.024	179.288	106.933	72.354
35°	141.990	176.282	94.605	81.677
	Centre Idler - Inbound of Junction			
	Average (kg)	Max (kg)	Min (kg)	Range (kg)
0°	160.447	220.482	99.912	120.570
15°	160.034	201.669	109.677	91.991
25°	154.924	183.812	119.968	63.845
35°	184.563	218.534	141.683	76.851

Table 7: Average data readings for the pseudo-dynamic 240 mm offset configuration

Trough Angle	**Wing Idler - Outbound of Junction**			
	Average (kg)	Max (kg)	Min (kg)	Range (kg)
0°	101.679	133.272	83.054	50.217
15°	127.161	160.454	95.984	64.469
25°	139.657	187.927	110.719	77.208
35°	138.138	174.870	91.463	83.408
	Centre Idler - Inbound of Junction			
	Average (kg)	Max (kg)	Min (kg)	Range (kg)
0°	152.832	225.860	92.233	133.627
15°	161.972	203.747	84.524	119.224
25°	162.030	211.839	108.981	102.857
35°	181.208	220.879	134.920	85.959